ORDER-ADAPTIVE FREQUENCY TRACKERS FOR DIRECT-TO-EARTH MARS COMMUNICATIONS

C. G. Lopes[♮], *E. Satorius*[‡], *P. Estabrook*[‡] *and A. H. Sayed*[†]

[♮] Electrical Engineering
Univ. of Sao Paulo, Brazil
cassio@lps.usp.br

[‡] Jet Propulsion Laboratory
Pasadena, CA
{Edgar.H.Satorius,Polly.Estabrook}@jpl.nasa.gov

[†]Electrical Engineering
UCLA, Los Angeles, CA
sayed@ee.ucla.edu

ABSTRACT

During the entry, descent and landing phase (EDL) of the missions to Mars, the spacecraft's high dynamics imprints severe Doppler swings on the signals transmitted via the direct-to-Earth (DTE) channel. In order to recover the data that record the mission status from the received signal, a reliable estimate of the Doppler profile is required. We extend previous work by developing order-adaptive schemes that enforce frequency continuity and improve tracking performance and, as a result, the overall frequency mean-square error as well.

Index Terms–Adaptive filters, adaptive order predictors, robust filtering, frequency estimation, Mars exploration.

1. INTRODUCTION

The most critical phase of the Mars missions is the entry, descent and landing (EDL). The high dynamics experienced by the landers during this phase translates into a combination of severe Doppler shifts in the carrier frequency and time-varying SNR [1] – see Fig. 1. During this time frame, flag signals that register the mission health are sent back to Earth in real time. In order to recover such signals, a reliable estimate of the Doppler swings is required.

In the typical EDL scenario, the low SNR levels allied with the fast dynamics may cause the appearance of frequency spikes in the estimated Doppler profile that do not reflect the lander dynamics. This is one of the main sources of errors and severely compromises the ability of the trackers to lock into the true frequency trajectory. In [1], this effect was treated by reprocessing the corresponding data block until lock is recovered.

In this work, an effective reprocessing strategy is devised based on order-adaptive predictors that attempt to enforce frequency continuity, improving performance as compared to existing fixed order adaptive linear predictors (ALP).

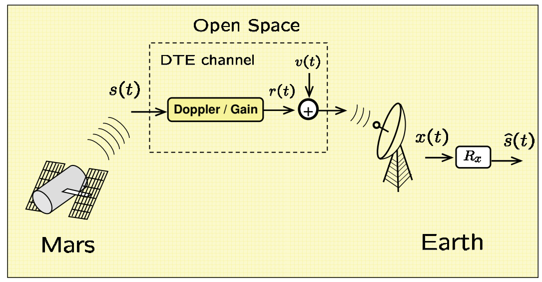

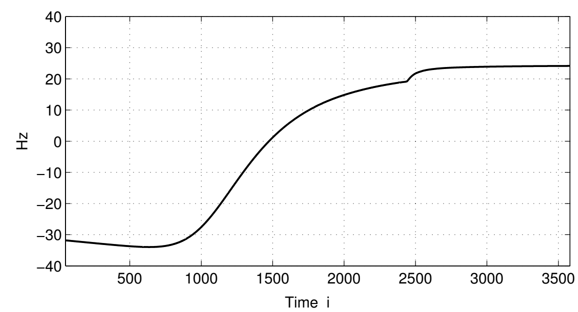

Fig. 1. Top: Direct-to-Earth communications. Bottom: typical EDL Doppler profile.

The new methods may be embedded in existing schemes to further enhance tracking performance [4, 5, 6].

2. EDL COMMUNICATIONS

The EDL events are flagged into the transmitted signal $s(t)$. At the Earth end, the received signal $x(t)$ is comprised of a distorted signal component $r(t)$ disturbed by noise $v(t)$, as illustrated in Fig. 1. A detailed description of the DTE channel and signal generation can be found in [1]. The signal is down-converted and sampled upon reception, so that it can be modeled as

$$x(i) = e^{j\phi(i)} + v(i)\,, \quad \phi(i) = 2\pi \sum_{k=0}^{i} f(k) \qquad (1)$$

This material was supported by the Jet Propulsion Laboratory under award 1276256 and by NSF awards ECS-0601266 and ECS-0725441. The first author was also supported by a fellowship from CAPES, Brazil, under award 1168/01-0.

where $f(i)$ is the discrete time-varying Doppler component and $v(i)$ arises from an ergodic white Gaussian noise process with variance σ_v^2. Our objective is to estimate and track $f(i)$ from measurements $\{x(i)\}$.

3. ADAPTIVE FREQUENCY TRACKERS

In the linear prediction approach to frequency tracking, an M^{th} order FIR predictor c generates the predicted signal

$$\hat{x}(i) = \sum_{k=1}^{M} c(k)x(i-k) \tag{2}$$

by minimizing the estimation error

$$e(i) = x(i) - \hat{x}(i) \tag{3}$$

in the least mean squares sense. The corresponding prediction-error filter $Q(z)$, defined by

$$Q(z) = 1 - \sum_{k=1}^{M} c(k)z^{-k} \tag{4}$$

is related to the input signal power spectral density, $S_x(e^{j\omega})$, via

$$S_x(e^{j\omega}) = \frac{K}{|Q(e^{j\omega})|^2} \tag{5}$$

which is a maximum entropy estimate, within a scaling factor K [2, 3]. Expression (1) indicates that the power spectrum of $x(i)$ is primarily comprised of a single peak, corresponding to the sinusoidal component, and the noise floor. The frequency corresponding to the peak is an estimate of the discrete Doppler frequency $f(i)$ [2, 3].

In the ALP approach, the predictor is designed by an adaptive algorithm [7]. Due to its robustness and simplicity [4], we employ a normalized least mean-squares (NLMS) predictor:

$$c_i = c_{i-1} + \mu \frac{x_{i-1}^*}{\|x_{i-1}\|^2 + \epsilon}\big(x(i) - x_{i-1}c_{i-1}\big) \tag{6}$$

where μ is a step-size and x_{i-1} is the regressor

$$x_{i-1} = [x(i-1)\; x(i-2)\; \cdots\; x(i-M+1)] \tag{7}$$

Therefore, at each time i, a discrete frequency estimate $\hat{f}(i)$ is retrieved from the adaptive predictor in (6) by seeking a peak in the corresponding S_x (or a notch in $|Q(e^{j\omega})|^2$).

4. ORDER-ADAPTIVE FREQUENCY TRACKERS

There are two main sources of errors in the frequency estimates. At high SNR, most of the error is caused by the estimation bias, which can be compensated using the techniques proposed in [5, 6]. At low SNR, the main source of error is the presence of frequency spikes, which are not correlated with the underlying true frequency and they contribute to a large fraction of the total frequency error. A simple and efficient locking scheme can be devised based on frequency temporal continuity, as detailed next.

4.1. Frequency continuity enforcement

The Doppler swings experienced by the carrier wave reflect directly the state of movement of the lander:

$$f(t) = \frac{f_c}{c} \cdot v_d(t) \tag{8}$$

where f_c is the nominal carrier frequency (Hz), c is the speed of light and $v_d(t)$ is the Doppler speed. Since it is not possible to alter instantaneously the linear momentum of any physical body, assuming that the spacecraft has constant mass, then its speed cannot vary abruptly. Consequently, from (8) we conclude that any spike observed in the frequency profile does not reflect the true Doppler component; in fact it is a manifestation of the ALP's sensitivity [4]–[6].

In Figure 2 we verify the sensitivity of the frequency trajectories for different predictor orders $M = 7, 11$, and 13, with $\mu = 0.11$, and SNR $= -7$dB. Different trackers experience spikes at different times. Hence, if we instantaneously pick the predictor whose order preserves frequency continuity at that time instant, the result is the bottom curve in Fig. 2: a spike-free frequency trajectory. [1]

4.2. Order-adaptive implementation

The previous section suggests that a predictor that seeks orders that preserve frequency continuity may improve considerably its tracking ability. The procedure has to be carried out on-the-fly though, thus bounds must be imposed on the order range to limit computational complexity and the appearance of false coherent trajectories [2]:

$$M(i) \in [M_{min}, M_{max}] \tag{9}$$

By doing so, we arrive at order-adaptive schemes that are able to maintain frequency lock in adverse scenarios. The question is *how* to implement such schemes without resorting to a pool of predictors as employed in Fig. 2.

Let us start by defining an update vector p_i in (6) as

$$p_i \;=\; \mu \frac{x_{i-1}^*}{\|x_{i-1}\|^2 + \epsilon}\big(x(i) - x_{i-1}c_{i-1}\big) \tag{10}$$

[1] The curve was obtained by searching predictors with odd order in the range $M = [7, 21]$ that preserved frequency continuity at every time i.

[2] For low SNR, if the order range is too wide, it is sometimes possible to find trajectories that preserve frequency continuity; however, they may not correspond to the actual frequency profile.

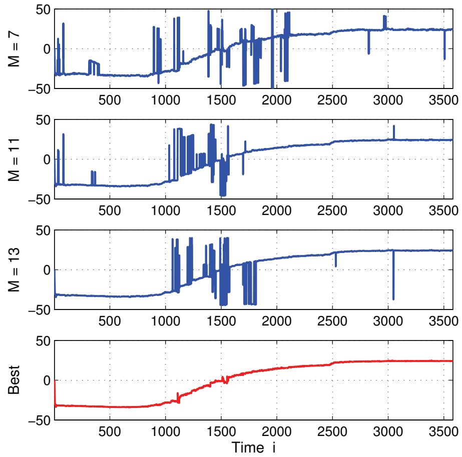

Fig. 2. Top three plots: sensitivity of the frequency trajectories. Bottom: estimates picked over different predictor orders.

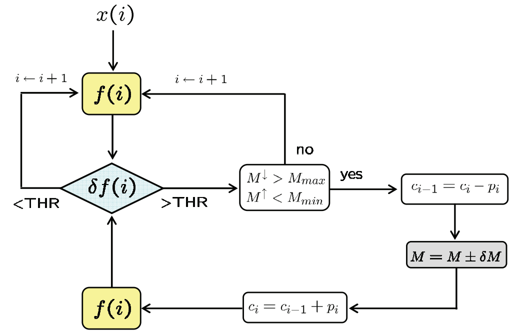

Fig. 3. Block diagram of the order-adaptive predictor.

which is parameterized in terms of filter order $M(i)$ and step-size μ.

Now, we proceed as follows. Considering the frequency estimate $\hat{f}(i-1)$ (assumed accurate), the frequency shift $\delta f = \hat{f}(i) - \hat{f}(i-1)$ and a pre-defined threshold THR, if at time i a frequency jump is detected ($\delta f > \text{THR}$), then the update p_i, with the current order $M(i)$, was the cause. We then remove the pathological update p_i from c_i, so that c_{i-1} is recovered. In the sequel, we change the system order $M(i)$, recalculate the new p_i and the corresponding predictor c_i, and retrieve the resulting new estimate $\hat{f}(i)$. If continuity is met ($\delta f < \text{THR}$), a new sample is processed, otherwise the procedure is repeated. The flowchart in Fig. 3 summarizes the principle of the order-adaptive procedure.

Depending on how the system order is adapted, different modes of operation are rendered. In this work we describe the *down* ($M^{\downarrow}$) and the *up* ($M^{\uparrow}$) modes.

4.3. Down mode

In the *down* mode, the filter operates initially with the upper bound order $M(i) = M_{max}$. If discontinuity in frequency is detected, the update vector p_i that resulted in the spike is removed. The *system*[3] order is then *reduced* according to some law. For instance

$$M(i) \leftarrow M(i) - \delta M \tag{11}$$

where δM is a positive integer. The newly order-reduced vector p_i is added to the order-reduced c_{i-1}, and the frequency estimate is retrieved again. If the continuity check is successful, the filter is restored to its original order and a new sample is processed. In case of check failure, the order is decreased until continuity is met or the lower bound M_{min} is reached. In this case, the lock is simply declared lost and pos-processing routines may be employed [4]–[6].

[3]The order of the previous predictor c_{i-1} has to be adjusted as well, in this case by truncating its δM trailing entries.

4.4. Up mode

The *up* mode complements the down mode: the predictor order is initialized with $M(i) = M_{min}$. In this mode, a pilot filter c'_i with order M_{max} is run independently, so that the order updating procedure is simplified. If frequency continuity is not met, the predictor order is *increased*:

$$M(i) \leftarrow M(i) + \delta M \tag{12}$$

The previous predictor c_{i-1}, which has a lower order, is then retrieved from the pilot filter, i.e., c_{i-1} is assigned with the $M(i)$ leading entries of c'_{i-1}:

$$c_{i-1} \leftarrow [c'_{i-1}]_{1:M(i)} \tag{13}$$

Once more, the new predictor c_i is calculated and frequency continuity is tested. If continuity is met, the predictor is restored to the original order and a new sample is processed. Otherwise, the order is increased until continuity is met, or the upper bound M_{max} is reached.

5. SIMULATIONS

Figures 4 and 5 show a single realization of the fixed order (with $M = M_{max}$) and the up and down order-adaptive schemes ($\delta M = 1$), with clear advantage in tracking performance for the order-adaptive predictors, both up and down. Parameters were chosen to allow meaningful comparison with previously proposed methods [4], [5]. Figure 6 compares the corresponding root mean-square frequency error for a wide SNR range. There is some advantage in favor of the down mode: even though the frequency continuity

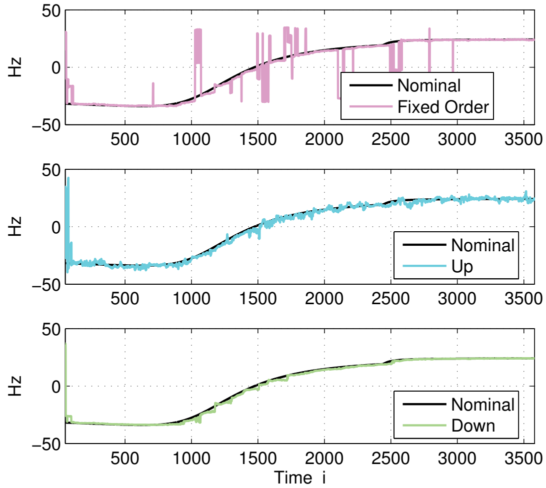

Fig. 4. Frequency estimates: original fixed order (top), the up and down modes. SNR = -8dB (12dB-Hz), $M_{min} = 5$, $M_{max} = 25$, $\delta M = 1$ and $\mu = 0.11$.

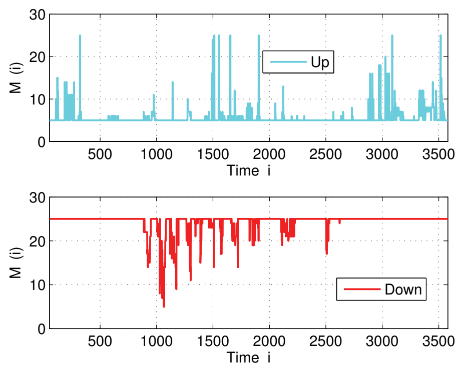

Fig. 5. Order evolution for Fig. 4: up and down modes.

may be met, longer filters are more efficient to combat the variance of the estimates.

Note that Fig. 5 confirms what would be expected from the up and down modes: during periods of high dynamics, the down mode will tend to be actively working to reduce the order, since shorter filters are able to react faster and tend to be less sensitive. The up mode, on the other hand, which usually operates near the lower bound M_{min}, will tend to present more order activity during low dynamics, since in such cases higher order filters may predict more efficiently the narrowband component $r(i)$.

6. CONCLUSION

We presented an order-adaptive scheme to combat frequency spikes taking place when tracking fast changing trajectories,

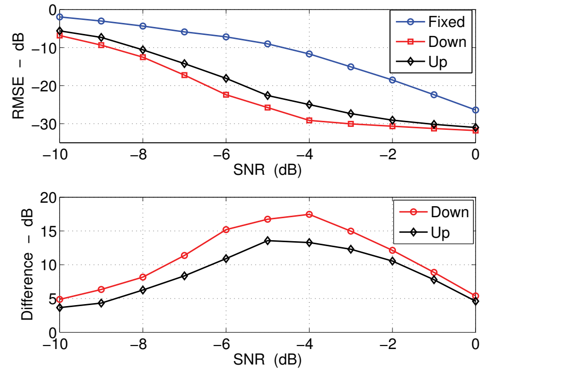

Fig. 6. The RMSE curves for fixed $M = M_{max} = 25$, up and down modes (same settings as in Fig. 4). The curves are normalized by the nominal profile $f(i)$ (in Hz).

particularly in low SNR scenarios. We focused on the improvement achieved when replacing a fixed order ALP by order-adaptive predictors that enforce frequency continuity. The new methods are also innovative if compared with typical variable order implementations [8, 9], which improve mean-square estimation, but not necessarily combat spikes, since they pursue different criteria.

7. REFERENCES

[1] W. J. Hurd, P. Estabrook, C. S. Racho, and E. Satorius. "Critical spacecraft-to-earth communications for Mars exploration rover (MER) entry, descent and landing,"*Proc. IEEE Aerospace Conference*, vol.3, pp. 1283-1292, MT, March 2002.

[2] L. J. Griffiths "Rapid Measurement of digital instantaneous frequency," *IEEE Trans. on Acoustics, Speech, and Signal Processing*, vol. ASSP-23, No. 2, pp. 207-222, April 1975.

[3] E. H. Satorius and J. R. Zeidler "Maximum entropy spectral analysis of multiple sinusoids in noise," *Proc. of Geophysics*, vol. 43, no.6, pp. 1111–1118, October 1978.

[4] C. G. Lopes, E. Satorius, A. H. Sayed. "Adaptive carrier tracking for Direct-to-Earth Mars communications," *Proc. of 40th Asilomar Conf. on Signals, Systems and Computers*, pp. 1042–1046, Pacific Grove, CA, Nov 2006.

[5] C. G. Lopes, P. Estabrook, E. H. Satorius, A. H. Sayed "Efficient adaptive carrier tracking for Mars to Earth communications during entry, descent and landing," *Proc. of IEEE Statistical Signal Processing Workshop*, Madison, pp. 517–521, Wisconsin, Aug. 2007.

[6] C. G. Lopes, E. H. Satorius, P. Estabrook, A. H. Sayed "Adaptive carrier tracking for Mars to Earth communications during entry, descent and landing," *IEEE Transactions on Aerospace and Electronic Systems*, 2009, *accepted*.

[7] A. H. Sayed. *Fundamentals of Adaptive Filtering*, Wiley, NJ, 2003.

[8] Z. Pritzker and A. Feuer, "Variable length stochastic gradient algorithm," *IEEE Trans. Signal Processing*, vol. 39, no. 4, pp. 997-1001, Apr. 1991.

[9] Y. Gu, K. Tang, H. Cui, and W. Du, "LMS algorithm with gradient descent filter length," *IEEE Signal Process. Lett.*, vol. 11, no. 3, pp. 305-307, Mar. 2004.